Stoichiometry for activation of neuronal α7 nicotinic receptors

Natalia Andersen[a], Jeremías Corradi[a], Steven M. Sine[b], and Cecilia Bouzat[a,1]

[a]Instituto de Investigaciones Bioquímicas, Universidad Nacional del Sur-Consejo Nacional de Investigaciones Científicas y Técnicas, 8000 Bahía Blanca, Argentina; and [b]Receptor Biology Laboratory, Departments of Physiology and Biomedical Engineering and Neurology, Mayo Clinic College of Medicine, Rochester, MN 55905

Edited by Richard W. Aldrich, University of Texas at Austin, Austin, TX, and approved November 4, 2013 (received for review August 20, 2013)

Neuronal α7 nicotinic receptors elicit rapid cation influx in response to acetylcholine (ACh) or its hydrolysis product choline. They contribute to cognition, synaptic plasticity, and neuroprotection and have been implicated in neurodegenerative and neuropsychiatric disorders. α7, however, often localizes distal to sites of nerve-released ACh and binds ACh with low affinity, and thus elicits its biological response with low agonist occupancy. To assess the function of α7 when ACh occupies fewer than five of its identical binding sites, we measured the open-channel lifetime of individual receptors in which four of the five ACh binding sites were disabled. To improve the time resolution of the inherently brief α7 channel openings, background mutations or a potentiator was used to increase open duration. We find that, in receptors with only one intact binding site, the open-channel lifetime is indistinguishable from receptors with five intact binding sites, counter to expectations from prototypical neurotransmitter-gated ion channels where the open-channel lifetime increases with the number of binding sites occupied by agonist. Replacing the membrane-embedded domain of α7 by that of the related 5-HT_3A receptor increases the number of sites that need to be occupied to achieve the maximal open-channel lifetime, thus revealing a unique interdependence between the detector and actuator domains of these receptors. The distinctive ability of a single occupancy to elicit a full biological response adapts α7 to volume transmission, a prevalent mechanism of ACh-mediated signaling in the nervous system and nonneuronal cells.

Cys-loop receptors | α7 nicotinic receptor | patch-clamp | agonist binding site | channel gating

The α7 acetylcholine nicotinic receptors (AChR) are among the most abundant AChRs in the central nervous system, where they are enriched in the medulla, pons, midbrain, thalamus, hippocampus, and cerebral cortex (1). They contribute to cognitive functioning, sensory information processing, attention, working memory, and reward pathways. Decline, disruption, or alterations of cholinergic signaling involving α7 have been implicated in various neurological diseases, such as schizophrenia, epilepsy, autism, Alzheimer's disease, and addiction (2–6). As a result, α7 has emerged as a novel therapeutic drug target (7, 8).

α7 are homomeric receptors from the Cys-loop family of pentameric ligand-gated ion channels. They are composed of three distinct modules: an extracellular domain that carries the agonist binding sites, a transmembrane domain that forms the ion-conducting pore, and an intracellular domain that contributes to ion conductance. They contain five identical binding sites, located at subunit interfaces in the extracellular domain (1, 9).

ACh binding leads to a series of conformational changes that open its cation-permeable transmembrane channel, followed by desensitization (10, 11). Hallmarks of α7 receptors include their high Ca^{2+} permeability, full activation by choline (a product of ACh hydrolysis), and extremely fast desensitization (12, 13). The allosteric mechanism by which binding of ACh mediates activation and desensitization remains a central question in the field.

Within the central nervous system, α7 receptors localize both pre- and postsynaptically, but they dominantly operate in an extrasynaptic mode (14). Choline is also an efficacious agonist of α7, which further extends the spatial range of cholinergic transmission. This combination of volume transmission and extension of bioactivity by choline is also relevant in nonneuronal cells, such as lymphocytes and macrophages, where α7 is involved in anti-inflammatory responses (15, 16), and in sperm cells where α7 has a role in fertilization (17).

α7 AChRs are thus physiological targets for both ACh and choline, but concentrations of these agonists are expected to be low and to change in proportion to overall neuronal activity, unlike at classical, on or off, fast cholinergic synapses. Furthermore, both ACh and choline bind to α7 with low affinity so that, under physiological conditions, agonist occupancy of the binding sites will be low. However, neurotransmitter-gated ion channels contain multiple agonist binding sites, and classical observations show that occupancy of multiple sites maximizes open-channel stability (11). Thus, we sought to compare open-channel stability of α7 with agonist bound to one or all five binding sites.

To this end, we generated α7 AChRs from two types of subunits, one that formed a disabled binding site and another that formed a normal binding site. To determine the number of intact binding sites in individual pentamers, we tagged one of the subunits with mutations that alter unitary conductance and then used patch-clamp recording to monitor the open channel lifetime of receptors with defined numbers of intact binding sites.

Significance

Nicotinic α7 receptors are neurotransmitter-gated ion channels that participate in cognitive, cytoprotective, and anti-inflammatory processes and have emerged as targets for neurological disorders and therapeutic drugs. They are associated with extrasynaptic volume transmission where they are exposed to low ACh concentrations and thus function with partial occupancy of their five identical binding sites. By generating α7 receptors with different numbers of functional ACh binding sites and measuring open-channel lifetimes of individual receptors, we find that occupancy of one site produces a maximal response and that the additional sites enhance agonist sensitivity. Thus, ACh occupancy of only one of five sites in α7 produces a maximal response, adapting it to extrasynaptic volume transmission in neuronal and nonneuronal cells.

Author contributions: N.A., J.C., S.M.S., and C.B. designed research; N.A., J.C., and C.B. performed research; S.M.S. contributed new reagents/analytic tools; N.A., J.C., and C.B. analyzed data; and S.M.S. and C.B. wrote the paper.

The authors declare no conflict of interest.

This article is a PNAS Direct Submission.

[1]To whom correspondence should be addressed. E-mail: inbouzat@criba.edu.ar.

This article contains supporting information online at www.pnas.org/lookup/suppl/doi:10.1073/pnas.1315775110/-/DCSupplemental.

Results

To gain insight into the relationship between binding-site occupancy by agonist and the overall response of α7, we coexpressed different mole ratios of α7 and α7 carrying the Y188T mutation, which prevents ACh binding but does not affect subunit assembly (18), and recorded whole-cell currents elicited by ACh.

For cells expressing the control human α7, a step pulse of ACh elicits a rapid increase of current that, in the continued presence of ACh, decays due to desensitization (Fig. 1*A*) (13). In contrast, ACh does not elicit measurable responses from α7-Y188T receptors (Fig. 1*B*). Responses from cells containing receptors formed by α7 and α7-Y188T subunits (subunit ratios 1:3 and 1:9 wt:wt) reach saturation at higher concentrations compared with α7 (Fig. 1*D*). Accordingly, dose–response curves from peak currents yield EC_{50} values of 140 ± 60 μM for α7 (nH: 1.2 ± 0.5, $n = 17$); 315 ± 47 μM for α7 + α7-Y188T 1:3 (nH: 1.2 ± 0.2, $n = 16$); and 410 ± 70 μM for α7 + α7-Y188T 1:9 (nH:1.3 ± 0.3, $n = 13$) (Fig. 1*D*).

At a saturating ACh concentration, the time course of onset of the inward current is indistinguishable between cells expressing α7 ($tr_{20–80}$ = 1.8 ± 1 ms) and α7 plus α7-Y188T ($tr_{20–80}$ = 2.3 ± 1 ms for 1:3 ratio, and $tr_{20–80}$ = 2.2 ± 0.7 ms for 1:9 ratio). These values approach the limit of the solution exchange time in our whole-cell recording system so that any difference would not be detectable. Similarly, at a saturating ACh concentration, the time course of decay from the peak current is similar between cells expressing α7 and α7 plus α7-Y188T. However, for subsaturating concentrations, both the onset and decay are faster for α7 compared with α7 plus α7-Y188T (Fig. 1 *A* and *C*).

Macroscopic currents result from the overall population of receptors in the cell and cannot distinguish contributions of receptors with different subunit stoichiometry. Nevertheless, in cells cotransfected with 1:3 or 1:9 ratios of α7 to α7-Y188T and assuming identical expression of both subunits, ~32–39% of receptors are expected to carry one functional binding site, but less than 0.1% to carry five sites. Thus, although receptors with fewer than five binding sites show reduced sensitivity to ACh, at saturation, the response is similar to that of receptors with all five binding sites (19).

To determine how the responses of individual receptors contribute to the macroscopic current responses, we again coexpressed α7 and α7-Y188T subunits (1:1 and 1:3 subunit ratios), but instead measured single-channel currents and compared open time distributions with those of the control α7. In the presence of 100–500 μM ACh, the control α7 exhibits single brief openings flanked by long closings, or less often, several openings in quick succession, known as bursts (Fig. 2*A*) (13). The open time distribution is described by the sum of two exponential components of 46 ± 3 μs and 230 ± 40 μs at 500 μM ACh ($n = 4$) (Fig. 2*A* and Table S1). The

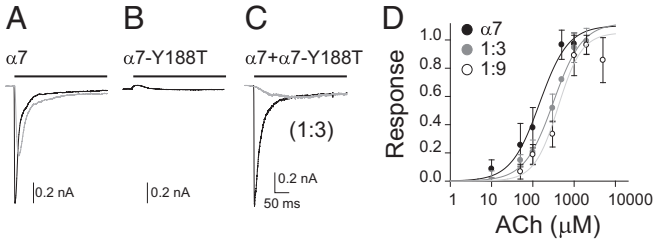

Fig. 1. Macroscopic responses of α7 with different average number of functional binding sites per receptor. Representative macroscopic responses to the application of a 300-ms pulse of 100 μM (gray line) or 1 mM ACh (black line) of cells expressing α7 (*A*) or receptors formed by α7 and α7-Y188T (subunit ratio 1:3) (*C*). No responses are elicited by 1 mM ACh from cells expressing α7-Y188T receptors (*B*). (*D*) Dose–response curves for α7 (●) and α7 + α7-Y188T receptors [1:3 (●) and 1:9 subunit ratios (○)]. Each point corresponds to the mean ± SD.

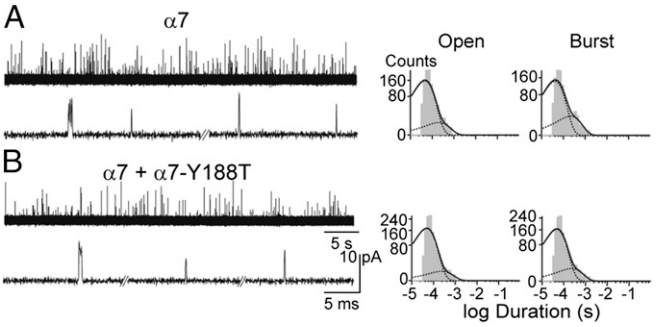

Fig. 2. Single-channel currents from cells transfected with α7 or mixed α7 + α7-Y188T subunits. Single-channel currents from cells transfected with α7 (*A*) or α7 and α7-Y188T (subunit ratio 1:3) (*B*) were recorded at −70 mV (500 μM ACh). Channel traces are shown at two different time scales. Typical open and burst duration histograms are shown for each condition. Openings are shown as upwards deflections.

mean burst duration is similar to the mean duration of the longest open component (240 ± 40 μs) (Table S1) (13). Single-channel openings were not detected from cells transfected with α7-Y188T subunits ($n = 19$ cell attached patches from green cells) whereas they were readily detected from cells transfected with both α7 and α7-Y188T subunits (Fig. 2*B*). For receptors containing wild-type and binding site mutant subunits, mean open durations were the same as those of the control α7 (mean duration of the longest component = 190 ± 20 μs and mean burst duration = 230 ± 20 μs for α7 plus α7-Y188T 1:3 subunit ratio; $n = 4$) (Fig. 2 and Table S1). Although these results suggest that open-channel lifetime is independent of the number of functional binding sites, the analyzed channel population comprises receptors with zero to five intact binding sites, but the number of intact sites in individual receptors is not known. What is needed is a means to directly register the subunit stoichiometry of individual receptors simultaneous with channel open duration.

We therefore applied an electrical fingerprinting strategy based on combining mutations that alter single-channel conductance with a mutation that prevents agonist binding. After coexpressing mutant and nonmutant subunits and recording agonist-evoked single-channel currents, the amplitude of each channel-opening event reports the number of intact binding sites in the pentamer whereas the dwell time indicates the stability of the open channel (18, 20, 21).

A crucial aspect of this strategy is the accurate measurement of single-channel amplitude, as it becomes the signature of receptor stoichiometry. However, single-channel openings from α7 exhibit a broad distribution of current amplitudes, and amplitude histograms cannot be fitted by a single Gaussian component (Fig. 3*A* and Fig. S1*A*). Simulation of single-channel currents, followed by filtering at different bandwidths, suggests that the appearance of multiple amplitudes mainly arises from limited time resolution of the inherently brief α7 openings (Fig. S2) (13). In agreement with this interpretation, an amplitude histogram constructed from channel openings with durations greater than 0.3 ms produces a single Gaussian distribution of amplitudes (Fig. 3*A*). Nonetheless a minor proportion of subconductance states cannot be excluded. Thus, an inherent limitation of α7 is that fully resolved openings comprise less than 4% of the total and would not be sufficient for the electrical fingerprinting strategy (Fig. S1*A*).

We therefore used background mutations or a potentiator to increase open channel lifetime. For the background mutant, we chose the PNU-insensitive quintuple mutant α7TSLMF because its mean open duration is longer than that of α7, but it retains normal ACh sensitivity and rapid desensitization (22). The mean duration of the longest open component is 0.90 ± 0.36 ms, and

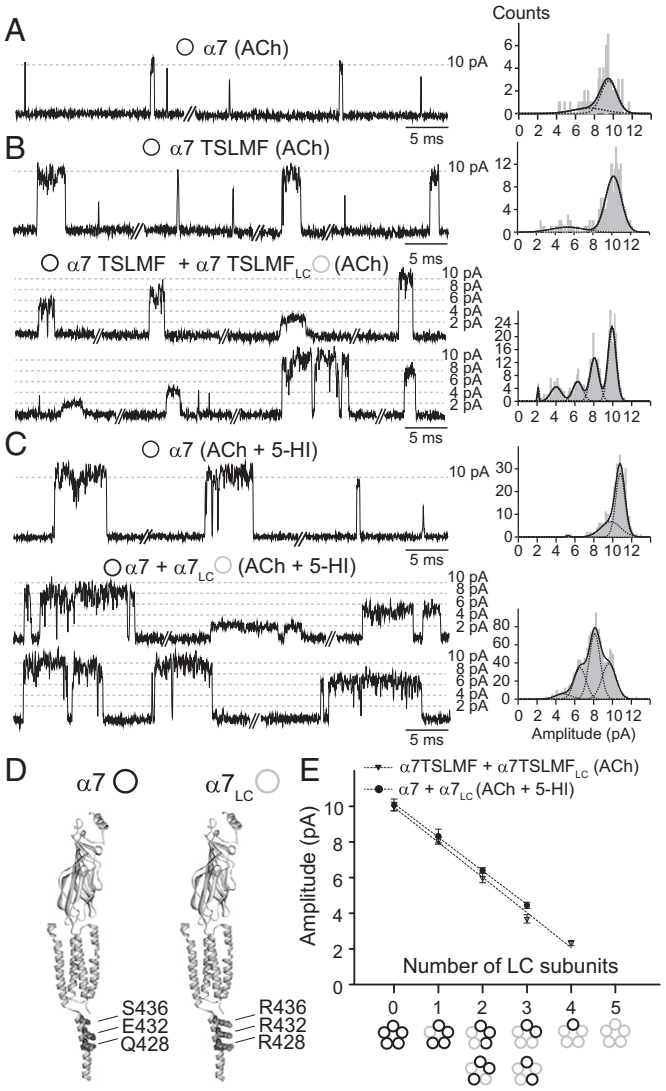

Fig. 3. Electrical fingerprinting for α7. (*A*) Single-channel currents activated by 100 μM ACh from wild-type α7. Amplitude histogram constructed with events longer than 0.3 ms. (*B*) Single-channel currents activated by 100 μM ACh from cells transfected with α7TSLMF alone (*Upper*) or together with α7TSLMF$_{LC}$ (*Lower*) (subunit ratio 1:1). (*C*) Single-channel currents activated by 100 μM ACh in the presence of 2 mM 5-HI from cells transfected with α7 alone (*Upper*) or together with α7$_{LC}$ (*Lower*) (subunit ratio 1:1). The two traces for the mixed subunits are excerpts from the same recording. Representative amplitude histograms are shown. Membrane potential: −70 mV. (*D*) Homology model of a single α7 subunit based on the Torpedo AChR structure (PDB ID code 2BG9), with the mutations that lead to the low-conductance form of α7 (α7$_{LC}$). (*E*) Plot of mean current amplitude against number of mutant low-conductance subunits. The fitted slopes are: 1.89 pA/LC subunit for α7 + α7$_{LC}$ in the presence of ACh + 5-HI and 1.97 pA/LC subunit for α7TSLMF + α7TSLMF$_{LC}$ in the presence of ACh. Note that α7 wild-type conductance is referred to as high conductance.

the mean burst duration is 1.60 ± 0.60 ms (n = 7) (Fig. 3*B* and Table S1). As for wild-type α7, amplitude histograms, restricted to openings with durations longer than 30 μs, span a wide range (Fig. S1). However, compared with α7, openings longer than 0.3 ms comprise a much larger fraction (22%) of the total (Fig. S1), resulting in a major Gaussian component of current amplitudes with a mean of ∼10 pA (Fig. 3*B*). Thus, this mutant becomes a useful tool for applying the electrical fingerprinting strategy.

Another means to increase open duration is to use a positive allosteric modulator (PAM). We chose the type I PAM, 5-hydroxyindole (5-HI) because it increases open and burst durations, but its effect is relatively subtle compared with the dramatic effect of the type II PAM PNU-120596 (22-24). In the presence of 100 μM ACh and 2 mM 5-HI, recordings from control α7 exhibit isolated openings or bursts of several successive openings (Fig. 3*C*). The mean durations of the longest component of openings (2.10 ± 0.20 ms) and bursts (5.10 ± 0.60 ms) are significantly prolonged with respect to α7 in the absence of PAM (n = 6) (Fig. S3 and Table S1). Amplitude histograms constructed for openings longer than 0.3 ms show a major Gaussian component of ∼10 pA at −70 mV (Fig. 3*C*).

The electrical fingerprinting strategy requires coexpression of low- and high-conductance subunits to generate receptors with different stoichiometry that can be distinguished by the single-channel amplitude. To this end, we generated an α7 low-conductance subunit by introducing three mutations in the intracellular M3–M4 region (Q428R, E432R, and S436R) (18, 21, 25). The triple mutant, or α7$_{LC}$ receptor, expresses well, and whole-cell ACh responses are identical to those from the control α7 (Fig. S4). However, because of its low conductance, single-channel openings cannot be detected from cell-attached patches (Fig. S4) (21).

Subunits that form receptors with normal conductance, referred to as high-conductance subunits, coassemble with low-conductance subunits to form receptors that exhibit discrete amplitude classes, as shown before (21). Recordings from cells transfected with α7TSLMF and α7TSLMF$_{LC}$ subunits, or α7 plus α7$_{LC}$ (in the presence of 100 μM ACh and 2 mM 5-HI) show openings with five discrete amplitude classes, indicating that each subunit contributes approximately equally to the single-channel conductance (Fig. 3 *B*, *C*, and *E* and Table S2). Thus, amplitude classes of 10, 8, 6, 4, and 2 pA correspond to receptors containing 0, 1, 2, 3, or 4 α7 low-conductance subunits (Fig. 3*E*). Thus, for each channel-opening episode, the single-channel current amplitude gives an instant register of the stoichiometry of high- and low-conductance subunits.

For both types of subunit-mixing experiments, α7TSLMF plus α7TSLMF$_{LC}$, or α7 plus α7$_{LC}$ in the presence of 5-HI, the mean open and burst durations are constant among amplitude classes (Table S2), indicating that the amplitude but not the lifetime is affected by the conductance mutations (18).

Having established methods to simultaneously register subunit stoichiometry and channel open time for individual receptors, we determined whether open-channel stability depends on the number of functional binding sites. We introduced the Y188T binding site mutation in α7TSLMF and α7 subunits and verified that channel activity was not detected from α7-Y188T receptors in the presence of 100 μM ACh and 2 mM 5-HI, or from α7TSLMF-Y188T receptors in the presence of 100–500 μM ACh (12-38 cell-attached patches from green fluorescent cells for each condition). We then transfected cells with both low- and high-conductance subunits, with or without the Y188T mutation, recorded single-channel currents, and compared mean open and burst durations for events corresponding to the 8-pA amplitude class, which arise from receptors containing one low-conductance and four high-conductance subunits (Fig. 3*E*). If the high-conductance subunit is either α7TSLMF or α7, openings from the 8-pA amplitude class correspond to receptors with five functional binding sites whereas, if the high-conductance subunit carries the Y188T mutation (α7TSLMF-Y188T or α7-Y188T), openings from the 8-pA amplitude correspond to receptors with only one functional binding site. Thus, in the two experiments, openings from the 8-pA amplitude class give information about receptors with either one or five functional binding sites.

The 8-pA openings, whether from receptors with either five or one functional binding site, show identical open-channel lifetimes (0.82 ± 0.26 and 0.72 ± 0.10 ms, respectively) and mean burst durations (1.20 ± 0.40 and 1.10 ± 0.55 ms, respectively, n = 6–8 for each condition) (Fig. 4*A* and Table S3). Analogously, in

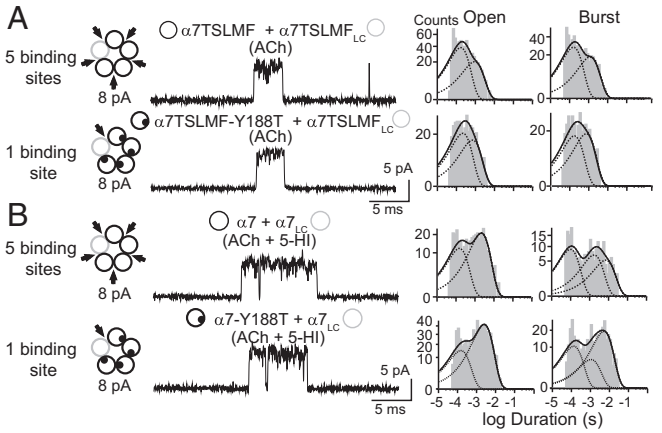

Fig. 4. Comparison of mean open and burst durations for α7 receptors containing five or one functional binding sites. Cells were transfected with α7TSLMF$_{LC}$ and α7TSLMF carrying (*Lower*) or not (*Upper*) the Y188T mutation (*A*) or with α7$_{LC}$ together with α7 (*Upper*) or α7-Y188T (*Lower*) (*B*). Single channels activated by 100 μM ACh in the absence (*A*) or presence of 2 mM 5-HI (*B*). The 8-pA amplitude class corresponds to receptors containing five or only one functional binding site (in the presence of Y188T mutation). Open and burst duration histograms are shown for each condition. Membrane potential: −70 mV.

the presence of 5-HI, openings from receptors containing either five (α7 and α7$_{LC}$ subunit mixture) or one functional binding site (α7-Y188T and α7$_{LC}$ subunit mixture) show identical open-channel lifetimes (2.30 ± 0.50 and 2.20 ± 0.70 ms, respectively) and burst durations (5.40 ± 1.40 ms and 5.10 ± 1.00 ms, respectively) (Fig. 4*B* and Table S3). A few 10-pA openings were detected in less than 20% of the patches in the presence of 5-HI although these openings were negligible compared with openings in the 8-pA amplitude class.

To further explore the relationship between the number of functional binding sites and open-channel lifetime, we analyzed receptors containing all possible numbers of binding sites by coexpressing α7-Y188T and α7$_{LC}$ or the reverse combination, α7 and α7$_{LC}$-Y188T, and recording ACh-activated channel openings in the presence of 2 mM 5-HI. Analysis of the different amplitude classes, which include pentameric arrangements containing from one to five functional binding sites, shows that mean open and burst durations are constant among receptors containing 1, 2, 3, 4, or 5 functional sites (Table S4).

We conclude that α7 AChRs can be activated if agonist occupies only one binding site and that open and burst durations are similar regardless of whether agonist occupies one or all five binding sites.

In contrast to α7, the open-channel lifetime of a receptor formed by the extracellular domain of α7 and the transmembrane region of 5-HT$_3$A (α7–5HT$_3$A) depends on the number of functional binding sites (18). For α7–5HT$_3$A receptors containing only one functional binding site, open and burst durations are briefer than those from receptors with three functional binding sites (18). The opposing occupancy–open lifetime relationships raise an interesting point because the binding domain is identical between the chimeric receptor and α7. Because openings of the chimera are long enough to allow full amplitude resolution, the electrical fingerprinting was performed in the absence of potentiators (18). We therefore explored whether, under identical conditions, i.e., in the presence of 5-HI, the relationship between binding-site occupancy and open-channel lifetime is also different between α7 and α7–5HT$_3$A receptors. For the electrical fingerprinting, we combined the high-conductance form of the chimera, which contains the triple QDA mutation (α7–5HT$_3$A$_{\mathbf{HC}}$) (25–28), and the original low-conductance form (α7–5HT$_3$A), which is electrically silent (18), and activated single channels by a saturating concentration of ACh (1 mM) (28). In the presence of 2 mM 5-HI, both openings and bursts are prolonged, confirming that 5-HI potentiates ACh-elicited currents from receptors containing the high-conductance form of α7–5HT$_3$A (Fig. S5) (28).

We next recorded single-channel currents in the presence of 1 mM ACh and 2 mM 5-HI from cells transfected with the α7–5HT$_3$A$_{\mathbf{HC}}$ (with or without the Y188T mutation) and the α7–5HT$_3$A subunit (low conductance), essentially as described before (18). Because the conductance of α7–5HT$_3$A$_{HC}$ receptors (90 pS) (28) is lower than that of α7, we increased the holding potential from −70 to −120 mV to better distinguish amplitude classes (18). We analyzed openings from the second highest amplitude class (7.9 ± 0.3 pA at −120 mV), corresponding to receptors containing four high-conductance subunits (18) and either five (in α7–5HT$_3$A$_{\mathbf{HC}}$ and α7–5HT$_3$A subunit mixture) or one (in α7–5HT$_3$A$_{\mathbf{HC}}$-Y188T and α7–5HT$_3$A subunit mixture) functional binding sites (Fig. 5).

5-HI produces open-channel block of the chimeric receptor, which decreases the mean open time in a voltage-dependent manner (Fig. S5). We therefore focused on burst durations that, in the absence of 5-HI, are significantly briefer in receptors containing one functional binding site than in those containing five (18). The results reveal that bursts from potentiated chimeric α7–5HT$_3$A receptors containing only one functional binding site (46 ± 15 ms, n = 11) are profoundly briefer than those from chimeric receptors containing five functional binding sites (126 ± 31 ms, n = 5) (Fig. 5). Thus, the occupancy–open time relationship diverges between α7 and α7–5HT$_3$A receptors, suggesting contributions of the pore domain or an interplay between the ligand binding and pore domains.

Discussion

The α7 nicotinic receptor is mainly involved in extrasynaptic or volume transmission where it is exposed to low concentrations of ACh or choline, and thus likely functions with partial occupancy of its five identical binding sites. To understand α7 function at submaximal occupancy, we took advantage of our previously established electrical fingerprinting strategy (18, 20, 21), which allows simultaneous measurements of the open-channel duration and the number of active binding sites in individual receptors in real time. A crucial requirement for this strategy is to fully resolve single-channel openings because the channel amplitude becomes the signature of receptor stoichiometry. Amplitude resolution is an inherent challenge for α7 because most channel openings are too brief to be fully resolved and thus do not reach

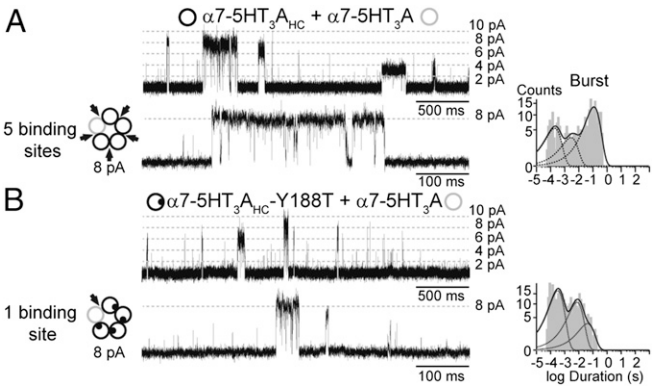

Fig. 5. Duration of bursts of α7–5-HT$_3$A containing five or one functional binding sites. Cells were cotransfected with control (α7–5HT$_3$A) and high-conductance (α7–5HT$_3$A$_{HC}$) subunits carrying (*B*) or not (*A*) Y188T mutation. Single channels were recorded in the presence of 1 mM ACh and 2 mM 5-HI at −120 mV. Channels of the amplitude class determined by four high-conductance subunits were analyzed, which correspond to arrangements containing five (*A*) or one (*B*) functional binding sites.

full amplitude. To obtain resolvable channel openings, we used two different tools to increase open duration: a background quintuple mutation and a type I PAM. The five residues in the α7TSLMF mutant outline an interhelical cavity to which the type II PAM, PNU-120596, binds; in addition to abolishing PNU potentiation, the mutations also increase open-channel duration in the absence of PNU, of which we took advantage (22). To provide an alternative means of increasing open time, we used the potentiator 5-HI. Because 5-HI is a type I PAM, its functional properties of modulation differ from those of type II PAMs, such as PNU (24, 29).

We demonstrate that occupancy of only one neurotransmitter binding site of α7 is sufficient for receptor activation and, unexpectedly, that it also achieves maximal open-channel lifetime. Increasing the number of functional binding sites from one to five does not lead to a concomitant increase in the stability of the open channel. The same result is obtained using two different experimental strategies, which supports our conclusion despite the inability to apply electrical fingerprinting to wild-type α7 in the absence of drugs.

Given the kinetic signature of α7 single-channel openings—absence of agonist concentration dependence and infrequent isolated openings—the channel-opening rate cannot be measured from single-channel recordings. However, at a saturating concentration of ACh, the onset of the macroscopic currents gives a lower limit of the rate of channel opening. Following a decrease in the number of functional binding sites, this rate remains indistinguishable from that of the control α7. Differences in the limiting rate may be further masked, however, by nonuniform agonist application, inherent to whole-cell measurements, together with the characteristic rapid desensitization of α7.

Thus, α7 activates well with one agonist bound, and channel gating may be similar for receptors with one and five functional binding sites, all this being a unique feature of α7. Maximal activation of α7 with submaximal occupancy was previously suggested from whole-cell current recordings (19).

The neuromuscular AChR has served as a model system to investigate mechanisms of operation of pentameric ligand-gated ion channels (11). The classical Monod, Wyman, and Changeux mechanism postulates that un-, mono-, and di-liganded AChRs undergo essentially the same global closed–open gating isomerization, and the agonist affinity ratio between closed and open states provides the energy to enhance gating with increased occupancy (30). Single-channel kinetic analysis of muscle AChRs has shown that the gating equilibrium constant increases with the number of bound ACh molecules (11, 31–33). Thus, our findings suggest that the occupancy–activation relationship differs among types of receptors in the Cys-loop family. For many receptor types, one agonist activates poorly but two or three activate well. This mechanism may protect against single occupancy activation at fast synapses where release sites are close to the postsynaptic receptors and to allow for rapid offset of synaptic responses. Other receptor types, such as α7, respond to low concentrations of ACh that change in a graded fashion; agonist occupancy of one site may trigger rearrangements within and between the subunits that are sufficient to destabilize the closed state and stabilize the open state. The diverging occupancy–activation relationship for the α7–5HT$_3$A chimera demonstrates that the transmembrane domain or the interface between the transmembrane and extracellular domains that differs between α7 and α7–5HT$_3$A (13), or an interplay with the ligand binding domain contribute to this relationship. It remains to be elucidated whether desensitization, which may contribute to α7 open-channel lifetime through a not yet fully known structural mechanism (10, 34–36), affects this relationship.

A previous study of competitive antagonism of α7 by methyllycaconitine (MLA) showed that, following wash out of MLA, recovery from inhibition followed a sigmoid rather than an exponential time course, suggesting that activation required dissociation of MLA from all five binding sites, in apparent contrast with our observation (37). However, the two observations can be reconciled by postulating that, whereas a single agonist occupancy is sufficient for activation, conformational change of the remaining four sites is also required, and MLA occupancy of these sites prevents conformational change and thus channel opening.

Previously, by applying the same electrical fingerprinting strategy to the α7–5HT$_3$A chimeric receptor, we showed that agonist occupancy of one binding site produces brief openings whereas occupancy of three sites produces much longer openings (18). Furthermore, we show here that, in the presence of 5-HI, α7–5HT$_3$A maintains the same occupancy–channel open time relationship. Because the extracellular domain of α7–5HT$_3$A is the same as that in α7, our results reveal a unique structural contribution to the occupancy–channel open time relationship: both the extracellular and pore domains are required. The extracellular domain is an obvious contributor, as it contains the ligand binding sites, but the pore domain alone, or in combination with the extracellular domain, also contributes. In the α7–5HT$_3$A chimera, the junction between the extracellular and pore domains contains mismatches where residues from α7 juxtapose residues from 5-HT$_3$A. Removing these mismatches, by installing either α7 or 5-HT$_3$A sequences, restores the single-channel kinetic signature of the corresponding parent receptor (13). Thus, the junction between extracellular β-sheet and transmembrane α-helical structures may contribute to the relationship between occupancy and open-channel lifetime.

Macroscopic responses of cells expressing mixed populations of receptors with a different number of functional binding sites show that the EC$_{50}$ increases as the number of intact binding sites per receptor decreases. Such increase may arise from an overall decrease in the rate of agonist association per receptor. A similar observation was reported for α7 (19) and α7–5HT$_3$A receptors (18). Thus, the availability of additional binding sites beyond that required for the maximal response enhances agonist sensitivity.

The enhanced sensitivity and activation by single-site occupancy make α7 ideal for extrasynaptic transmission in brain as well as in nonneuronal cells where it likely functions with submaximal occupancy. In addition, its brief open duration may be a protective mechanism against calcium-mediated toxicity. Thus, the activation mechanism of α7 seems adapted to unique and diverse physiological roles, including cytoprotective, anti-inflammatory, and cognitive functions.

Materials and Methods

Additional experimental procedures are described in *SI Materials and Methods*.

Site-Directed Mutagenesis and Expression of Receptors. The low-conductance form of α7 (α7$_{LC}$) was constructed by mutating the homologous residues to arginine residues (Q428R, E432R, S436R) (21). The α7 wild-type conductance is referred to as "high conductance." The high-conductance form of α7–5HT$_3$A was obtained by substitution of three arginine residues (R432Q, R436D and R440A) (18, 27, 28) whereas the original form is referred to as "low conductance." The α7 quintuple mutant carries five substitutions within transmembrane domains (S223T, A226S, M254L, I281M and V288F) (22). BOSC 23 cells were transfected by calcium phosphate precipitation as described previously with subunit cDNAs together with Ric-3 cDNA for cell-surface expression (13, 27).

Single-Channel Recordings. Single-channel recordings were obtained in the cell-attached patch configuration (13). For α7, the bath and pipette solutions contained 142 mM KCl, 5.4 mM NaCl, 1.8 mM $CaCl_2$, 1.7 mM $MgCl_2$, and 10 mM Hepes (pH 7.4). ACh alone or in the presence of 2 mM 5-hydroxyindole (5-HI) was added to the pipette solution. For α7–5HT$_3$A, the bath and pipette solutions contained 142 mM KCl, 5.4 mM NaCl, 0.2 mM $CaCl_2$, and 10 mM Hepes (pH 7.4) (28).

Single-channel currents were digitized at 5- to 10-μs intervals, low-pass filtered at a cutoff frequency of 10 kHz using an Axopatch 200 B patch-clamp amplifier (Molecular Devices), and analyzed using the program TAC with the Gaussian digital filter at 9 kHz (final cutoff frequency 6.7 kHz)

(Bruxton) (27). Open-time histograms were fitted by the sum of exponential functions by maximum likelihood using the program TACFit (Bruxton).

Electrical Fingerprinting. To define amplitude classes from receptors generated by coexpression of high- and low-conductance subunits, analysis was performed by tracking events regardless of current amplitude. Amplitude histograms were then constructed, and the different amplitude classes were distinguished. To determine the mean open and burst durations of each amplitude class, the analysis was performed in two different ways (18). In one, all opening events were detected without any restriction of amplitude. Open time histograms were then constructed for a given amplitude class by selecting only openings with amplitudes of ±0.6 pA of that of the mean of the class. In the second way, only openings whose amplitudes were between ±0.6 pA of that of the mean amplitude class under study were accepted during the detection. The corresponding duration histogram was then constructed from the accepted events (18). No significant differences in the mean durations were observed between the two types of analyses. Bursts of openings were identified as a series of closely separated openings preceded and followed by closings longer than a critical duration, typically 300–500 μs for α7, 1–2 ms for α7TSLMF, 1–3 ms for α7 in the presence of 5-HI, and 2–5 ms for α7–$5HT_3$A.

Macroscopic Current Recordings. Currents were recorded in the whole-cell configuration. The pipette solution contained 134 mM KCl, 5 mM EGTA, 1 mM $MgCl_2$, and 10 mM Hepes (pH 7.3). The extracellular solution (ECS) contained 150 mM NaCl, 1.8 mM $CaCl_2$, 1 mM $MgCl_2$, and 10 mM Hepes (pH 7.3). We applied a 300-ms pulse of ECS containing ACh at different concentrations (13). Currents were filtered at 5 kHz, digitized at 20 kHz, and analyzed using the IgorPro software (WaveMetrics). Each current represents the average from three to five individual traces obtained from the same cell. The rise time of the currents (tr_{20-80}) was determined by calculating the time in which the current increased from 20% to 80% of the peak. EC_{50} was calculated from dose–response curves by nonlinear regression analysis using the Hill equation: $R/Rmax = 1/[1+(EC_{50}/L)^{nH}]$, where EC_{50} is the agonist concentration that elicits the half-maximal response, nH is the Hill coefficient, and L is the agonist concentration.

ACKNOWLEDGMENTS. We thank Dr. N. Mukhtasimova, Dr. C. daCosta, and Mr. C. Free (Mayo Clinic) for helpful comments and providing mutants. This work was supported by grants from Universidad Nacional del Sur, Agencia Nacional de Promoción Científica y Tecnológica, and Consejo Nacional de Investigaciones Científicas y Técnicas de Argentina (to C.B.) and by National Institutes of Health Grant NS031744 (to S.M.S.).

1. Millar NS, Gotti C (2009) Diversity of vertebrate nicotinic acetylcholine receptors. *Neuropharmacology* 56(1):237–246.
2. Dani JA, Bertrand D (2007) Nicotinic acetylcholine receptors and nicotinic cholinergic mechanisms of the central nervous system. *Annu Rev Pharmacol Toxicol* 47:699–729.
3. Thomsen MS, Hansen HH, Timmerman DB, Mikkelsen JD (2010) Cognitive improvement by activation of alpha7 nicotinic acetylcholine receptors: From animal models to human pathophysiology. *Curr Pharm Des* 16(3):323–343.
4. Wallace TL, Porter RH (2011) Targeting the nicotinic alpha7 acetylcholine receptor to enhance cognition in disease. *Biochem Pharmacol* 82(8):891–903.
5. Hurst R, Rollema H, Bertrand D (2013) Nicotinic acetylcholine receptors: From basic science to therapeutics. *Pharmacol Ther* 137(1):22–54.
6. Wallace TL, Bertrand D (2013) Alpha7 neuronal nicotinic receptors as a drug target in schizophrenia. *Expert Opin Ther Targets* 17(2):139–155.
7. Haydar SN, Dunlop J (2010) Neuronal nicotinic acetylcholine receptors: Targets for the development of drugs to treat cognitive impairment associated with schizophrenia and Alzheimer's disease. *Curr Top Med Chem* 10(2):144–152.
8. Pohanka M (2012) Alpha7 nicotinic acetylcholine receptor is a target in pharmacology and toxicology. *Int J Mol Sci* 13(2):2219–2238.
9. Bouzat C (2012) New insights into the structural bases of activation of Cys-loop receptors. *J Physiol Paris* 106(1-2):23–33.
10. Corringer PJ, et al. (2012) Structure and pharmacology of pentameric receptor channels: From bacteria to brain. *Structure* 20(6):941–956.
11. Sine SM (2012) End-plate acetylcholine receptor: Structure, mechanism, pharmacology, and disease. *Physiol Rev* 92(3):1189–1234.
12. Mike A, Castro NG, Albuquerque EX (2000) Choline and acetylcholine have similar kinetic properties of activation and desensitization on the alpha7 nicotinic receptors in rat hippocampal neurons. *Brain Res* 882(1-2):155–168.
13. Bouzat C, Bartos M, Corradi J, Sine SM (2008) The interface between extracellular and transmembrane domains of homomeric Cys-loop receptors governs open-channel lifetime and rate of desensitization. *J Neurosci* 28(31):7808–7819.
14. Lendvai B, Vizi ES (2008) Nonsynaptic chemical transmission through nicotinic acetylcholine receptors. *Physiol Rev* 88(2):333–349.
15. De Rosa MJ, Dionisio L, Agriello E, Bouzat C, Esandi MdelC (2009) Alpha 7 nicotinic acetylcholine receptor modulates lymphocyte activation. *Life Sci* 85(11-12):444–449.
16. Andersson U, Tracey KJ (2012) Reflex principles of immunological homeostasis. *Annu Rev Immunol* 30:313–335.
17. Jaldety Y, et al. (2012) Sperm epidermal growth factor receptor (EGFR) mediates α7 acetylcholine receptor (AChR) activation to promote fertilization. *J Biol Chem* 287(26): 22328–22340.
18. Rayes D, De Rosa MJ, Sine SM, Bouzat C (2009) Number and locations of agonist binding sites required to activate homomeric Cys-loop receptors. *J Neurosci* 29(18): 6022–6032.
19. Williams DK, Stokes C, Horenstein NA, Papke RL (2011) The effective opening of nicotinic acetylcholine receptors with single agonist binding sites. *J Gen Physiol* 137(4):369–384.
20. Andersen N, Corradi J, Bartos M, Sine SM, Bouzat C (2011) Functional relationships between agonist binding sites and coupling regions of homomeric Cys-loop receptors. *J Neurosci* 31(10):3662–3669.
21. daCosta CJ, Sine SM (2013) Stoichiometry for drug potentiation of a pentameric ion channel. *Proc Natl Acad Sci USA* 110(16):6595–6600.
22. daCosta CJ, Free CR, Corradi J, Bouzat C, Sine SM (2011) Single-channel and structural foundations of neuronal α7 acetylcholine receptor potentiation. *J Neurosci* 31(39): 13870–13879.
23. Zwart R, et al. (2002) 5-Hydroxyindole potentiates human alpha 7 nicotinic receptor-mediated responses and enhances acetylcholine-induced glutamate release in cerebellar slices. *Neuropharmacology* 43(3):374–384.
24. Grønlien JH, et al. (2007) Distinct profiles of alpha7 nAChR positive allosteric modulation revealed by structurally diverse chemotypes. *Mol Pharmacol* 72(3):715–724.
25. Corradi J, Gumilar F, Bouzat C (2009) Single-channel kinetic analysis for activation and desensitization of homomeric 5-HT(3)A receptors. *Biophys J* 97(5):1335–1345.
26. Kelley SP, Dunlop JI, Kirkness EF, Lambert JJ, Peters JA (2003) A cytoplasmic region determines single-channel conductance in 5-HT3 receptors. *Nature* 424(6946): 321–324.
27. Bouzat C, et al. (2004) Coupling of agonist binding to channel gating in an ACh-binding protein linked to an ion channel. *Nature* 430(7002):896–900.
28. Rayes D, Spitzmaul G, Sine SM, Bouzat C (2005) Single-channel kinetic analysis of chimeric alpha7-5HT3A receptors. *Mol Pharmacol* 68(5):1475–1483.
29. Williams DK, Wang J, Papke RL (2011) Positive allosteric modulators as an approach to nicotinic acetylcholine receptor-targeted therapeutics: Advantages and limitations. *Biochem Pharmacol* 82(8):915–930.
30. Monod J, Wyman J, Changeux JP (1965) On the nature of allosteric transitions: A plausible model. *J Mol Biol* 12:88–118.
31. Bouzat C, Barrantes F, Sine S (2000) Nicotinic receptor fourth transmembrane domain: Hydrogen bonding by conserved threonine contributes to channel gating kinetics. *J Gen Physiol* 115(5):663–672.
32. Nayak TK, Purohit PG, Auerbach A (2012) The intrinsic energy of the gating isomerization of a neuromuscular acetylcholine receptor channel. *J Gen Physiol* 139(5):349–358.
33. Auerbach A (2013) The energy and work of a ligand-gated ion channel. *J Mol Biol* 425(9):1461–1475.
34. Zhang J, et al. (2011) Desensitization of alpha7 nicotinic receptor is governed by coupling strength relative to gate tightness. *J Biol Chem* 286(28):25331–25340.
35. Keramidas A, Lynch JW (2013) An outline of desensitization in pentameric ligand-gated ion channel receptors. *Cell Mol Life Sci* 70(7):1241–1253.
36. Zhang J, Xue F, Liu Y, Yang H, Wang X (2013) The structural mechanism of the Cys-loop receptor desensitization. *Mol Neurobiol* 48(1):97–108.
37. Palma E, Bertrand S, Binzoni T, Bertrand D (1996) Neuronal nicotinic alpha 7 receptor expressed in Xenopus oocytes presents five putative binding sites for methyllycaconitine. *J Physiol* 491(Pt 1):151–161.